Planar Laser Induced Fluorescence (PLIF) Flow Visualization applied to Agricultural Spray Nozzles with Sheet Disintegration; Influence of an Oil-in-Water Emulsion

Michael D. Cloeter[*1], Kuide Qin[2], Pramod Patil[1], Billy Smith[1]
[1]The Dow Chemical Company, Core R&D, Fluid Mechanics & Mixing Discipline, Freeport, TX
[2]Dow AgroSciences LLC, Crop Protection R&D, Indianapolis, IN

Abstract

A typical agricultural spray process involves atomizing a liquid stream of diluted pesticide solution through hydraulic spray nozzles that inherently produce a wide spectrum of spray droplet sizes. Finer droplets have higher potential for off-target movement or drift, which is of concern due to their potential impacts on neighboring crops and livestock, sensitive ecological resources, and human health. A factor that has been found to reduce fines production is the addition of an oil phase in the form of an oil-in-water emulsion. The mechanism of the effect is not fully understood.

The flow visualization technique Planar Laser Induced Fluorescence (PLIF) is commonly employed for characterization of scalar mixing. PLIF has also been used to characterize sprays. For this study, Rhodamine WT fluorescent dye was mixed into the solution to be sprayed. The laser sheet, aligned vertically, is passed through the exit area of the nozzle causing the droplets to fluoresce. The fluoresced pattern is imaged. For sprays, image pairs are taken on the order of 100 µs apart, thus the displacement and hence velocity vectors of drops can be computed throughout the spray pattern. Additionally, the images are of sufficient quality to study liquid sheet breakup physics.

For sprays with sheet breakup, such as many fan-type agricultural sprays, PLIF is effective at measuring the velocity within the spray before, during, and after the sheet disintegration. The motion of surface features on the sheet before disintegration allow the velocity to be calculated in a similar fashion to discrete particles. Traditional Particle Image Velocimetry (PIV) can in principle work as well, however the image quality from light scattered off of the unbroken sheet in PIV was found to be inferior to images from fluoresced light generated within the sheet by PLIF.

The method was applied to fan sprays (hydraulic and air-induced) in common use in agricultural applications. Measurements were performed with and without an emulsifiable methylated soybean oil concentrate phase. Velocity profiles were shown to be consistent with patternation data taken via a mechanical collection method. It was shown that the oil phase has a large impact on velocity profile. The effect of the emulsion on liquid sheet breakup physics was elucidated from the PLIF imaging.

[*] Corresponding Author: mcloeter@dow.com

Introduction

A typical agricultural spray process involves atomizing a liquid stream of diluted pesticide solution through hydraulic spray nozzles that inherently produce a wide spectrum of spray droplet sizes. Finer droplets have higher potential for off-target movement or drift, which is of concern due to their potential impacts on neighboring crops and livestock, sensitive ecological resources, and human health. A factor that has been found to reduce fines production is the addition of an oil phase in the form of an oil-in-water emulsion.

The mechanism of the emulsion effect is not fully understood. Hence, a rigorous experimental program was undertaken in order to more fully understand the performance of hydraulic and air induction nozzles, specifically in the context of fines production, related to the oil-in-water emulsion. Measurements were performed with and without an additive called InterLock®, an emulsifiable methylated soybean oil concentrate phase (www.agrisolutionsinfo.com). The nozzle types were a Teejet® 8002, annotated as "8002", and a Teejet® AI9502EVS, annotated as "AI9502".

The data reported here include droplet size distribution, patternation via a tray system, and planar laser induced fluorescence (PLIF) for velocity distribution. The PLIF analysis of the spray near the sheet breakup region is insightful for understanding the mechanism of drop formation and observing pertinent dynamics.

The next section of this report describes all of the experimental methods that were used. This is followed by a section on results, followed by conclusions.

Experimental Methods

Two test nozzles used in this study are shown in Figure 1. The 8002 is a purely hydraulic nozzle, whereas the AI9502 uses air induction through holes in the liquid feed line to create bubble-filled drops. A backpressure of 40 psi was used throughout this study, giving flows of 1.26×10^{-5} m^3/s (0.20 gpm) for both nozzles.

Figure 1. Images showing spray nozzles used in the study. Left, hydraulic Teejet® 8002, Right, Air Induction Teejet® AI9502EVS.

Figure 2 shows a schematic of the experimental apparatus used for this spray study.

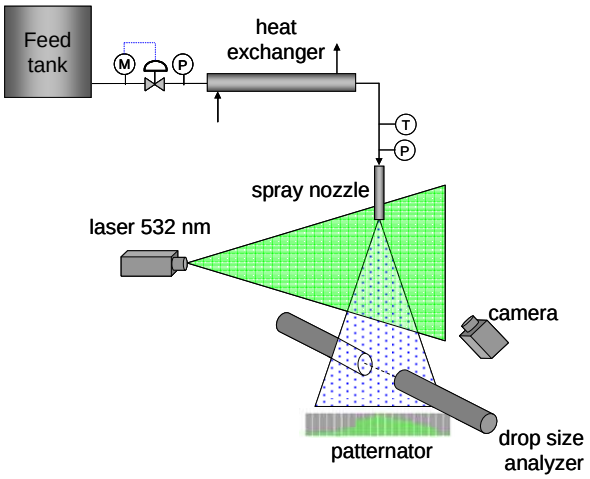

Figure 2. Schematic of the lab rig used for spray analysis showing the analytical methods used.

Both Particle Image Velocimetry (PIV) and PLIF have been used in many projects in the authors' laboratory. A complete overview of these methods can be found elsewhere [1, 2, 3], including for sprays [4, 5]. For this experimentation, a Dantec Dynamics FlowMap System Hub running FlowManager 4.60 was used to coordinate information flow between the lasers, cameras, and desktop computer. The dual lasers are New Wave Research Gemini (Nd:YAG) with energy of 120 mJ/pulse. Cylindrical optics are used to convert the laser beam to a laser sheet that is passed through the flow region of interest. As illustrated in Figure 2, the laser sheet is oriented parallel to the spray through the center of the flat fan pattern. The PLIF camera is a PCO SensiCam 12-bit monochrome digital CCD camera.

A fluorescent dye (Rhodamine WT) is added to the incoming feed stream. This dye fluoresces to a pink color as the solution passes through the laser. The PLIF camera is outfitted with a red filter and mounted perpendicular to the laser sheet to capture images of the fluorescent dye pattern at rates up to 7.5 Hz. As practiced the spatial resolution is on the order of 100 microns. By taking separate images a short time interval apart (100 µs in this study), velocity vectors are calculated. This is illustrated in Figure 3.

This work combines attributes of both PIV and PLIF. Traditionally, PIV is used for tracking movements of groups of seed particles over known time intervals and converting this information to a velocity vector field. Light scattering off of the seed particles is used in the imaging. PLIF is traditionally used in mixing experiments where a fluorescent dye solution is tracked as it mixes with a second fluid.

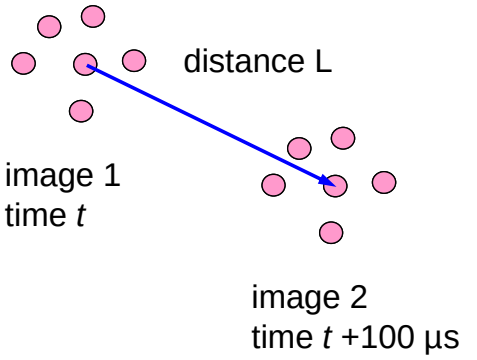

Figure 3. Concept used for generation of the velocity field in a spray.

For spray systems, the droplets themselves can be used for tracking. For multiphase systems, light-scattering optical methods such as traditional PIV can be problematic due to the irregular reflection of laser light off of the sheet and drop surfaces. By using the fluoresced light, characteristic of PLIF, higher quality images are obtained. Scattered laser light is filtered out by the red camera filter. Furthermore, for flat fan spray nozzles of the type discussed here, the movement of surface features of the sheet before and during disintegration can be tracked and converted to velocity vectors.

Figure 4 shows an image from a PLIF experiment in progress for a spray nozzle. The green color of the spray is caused by light scattering of the green laser.

Figure 4. Photograph taken during a PLIF imaging experiment.

Patternation measurements were conducted by allowing the spray to flow into compartments for a given amount of time until the fastest-rising compartment is almost full. Customarily, a single row of compartments is used. For this work, several rows of ½" x ½" cuvettes were used to gather a 3-dimensional data set for each fan spray. The distance between the nozzle tip and patternator was kept constant at 12 inches. After an experiment, the contents of each cell were individually weighed. The results were converted to a flux and plotted for visual analysis.

For drop size distribution measurement, dynamic imaging analysis is used. A small cross-section of the spray, approximately 5 mm square, is imaged using CCD camera on one side and a strobe on the other side as backlighting. The short duration of the strobe causes the individual droplets to appear locked in position, without streaks. The velocity of the droplets is sufficient that there is no cross-correlation between adjacent images, i.e. droplets are counted only once.

Throughout this imaging, automated processing is conducted to remove out-of-focus droplets as well as those that are cut off by the edge of the image. For this work, a sufficient number of images is collected to total at least 80,000 valid droplets. The diameter of each valid droplet is measured and used to generate common spray statistics including the volume-to-surface-area mean (Sauter mean, d_{32}), volume median (D_{50}), a measure of the largest particles below which 90% of the mass is present (D_{90}), and finally the mass fraction of driftable fines, defined to be droplets less than 100 µm (x_{fines}).

For experiments with emulsions, a 1000 ppm emulsion of methylated soybean oil (InterLock®) in deionized water was prepared in four gallon batches. A simple lab hydrofoil mixer was used to disperse the oil phase. The oil is self-emulsifying so no high-shear device was required. The oil solution was used within a few days after preparation. The viscosity of the oil phase is 0.0053 Pa-s. The median diameter, D_{50}, of the emulsion droplets was measured as 16 µm with a span of 1.8 using a Malvern Mastersizer 2000 laser diffraction particle analyzer.

Results

In this section the results of PLIF imaging (sample images and vector fields) and patternation are shown first for the 8002 and then for the AI9502 nozzle. In each case, figures are shown side-by-side with pure water (no emulsion) and with the emulsion present. Figure 5, Figure 6, and Figure 7 show the respective data for the 8002.

In Figure 5, the two sample PLIF images clearly show the sheet breakup regions without and with the emulsion present. Attributes of perforation and wave phenomena are evident. It is clear that the effect of the emulsion is to shrink the area of the breakup quite substantially, as is illustrated by the red boundaries added to Figure 5.

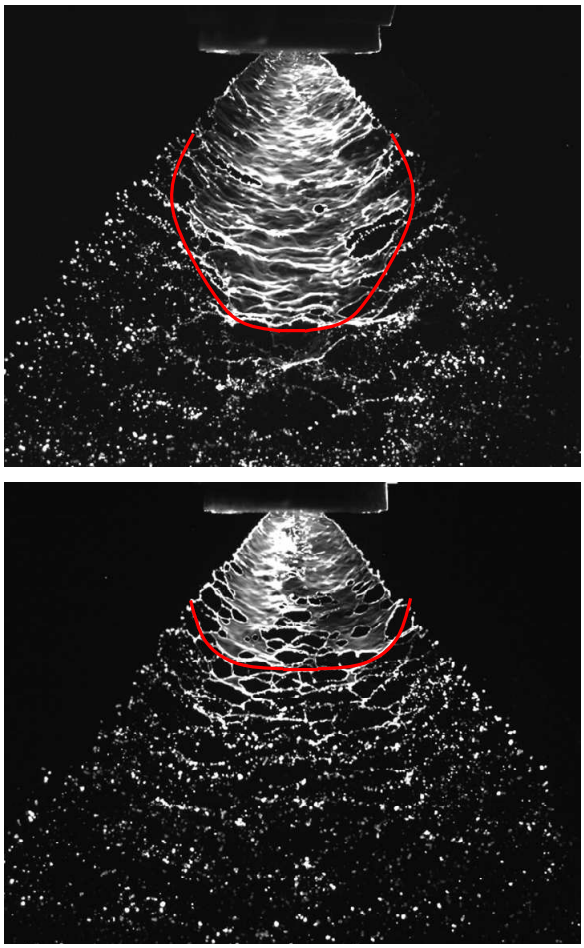

Figure 5. Sample images at 40 psi backpressure (flow 1.26×10^{-5} m^3/s) with 8002 nozzle. Top image, water only. Bottom image, with 1000 ppm InterLock® emulsion. Red lines annotate approximate boundary of initial sheet disintegration.

The 8002 exit orifice is elliptical with dimensions of 0.59 mm x 1.36 mm as measured via microscopy in the authors' laboratory. At the volumetric flow of 1.26×10^{-5} m^3/s, the average tip velocity of the liquid at the orifice is calculated as 20.5 m/s.

Figure 6 shows the results of PLIF velocimetry experimentation for 8002 sprays without and with the emulsion phase. Velocity vectors are overlayed on a contour plot colored by velocity magnitude that were derived through the averaging of 500 PLIF images. The measured velocities in the range of 18 – 21.5 m/s are quite consistent with the calculated average value of 20.5 m/s, keeping in mind that the actual fan spray has some three-dimensional character.

From Figure 6 it is immediately obvious that the emulsion causes a significant change in the velocity profile for the 8002 in comparison to pure water. The effect in the center plane shown is to spread out the region of high velocity, in essence reducing the deceleration shown in the top image. The area of highest velocity from the water-only plot overlays approximately the unbroken sheet, whereas with the emulsion the highest velocity region is spread out well after the breakup of the sheet. This can potentially be attributed, at least in part, to a change in the drop size distribution that has modified the droplet drag. As well, evident in the top plot of Figure 6 are "arms" near the boundary of the spray field with higher velocity than portions of the interior. These aren't as distinguishable with the emulsion.

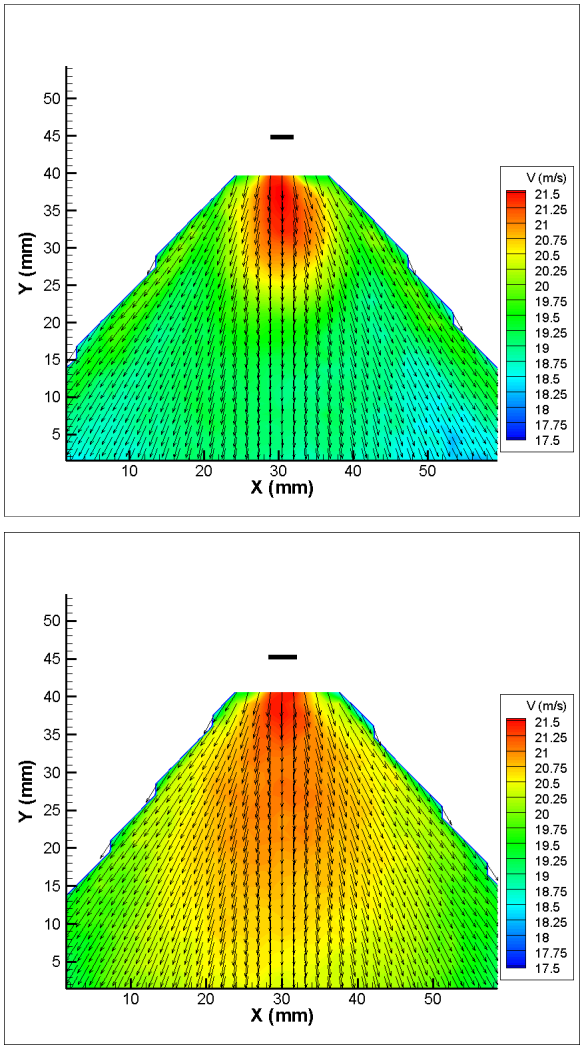

Figure 6. Velocity vectors with contour plot colored by velocity magnitude for 8002 nozzle with flow conditions same as Figure 5. Top plot, water only. Bottom plot, with 1000 ppm InterLock® emulsion.

Figure 7 shows results of patternation measurements for the 8002 sprays without and with the emulsion phase. The effect of the emulsion is shown to

reduce the flux of mass to the shoulders of the spray. This is consistent with the velocity profiles shown in Figure 6.

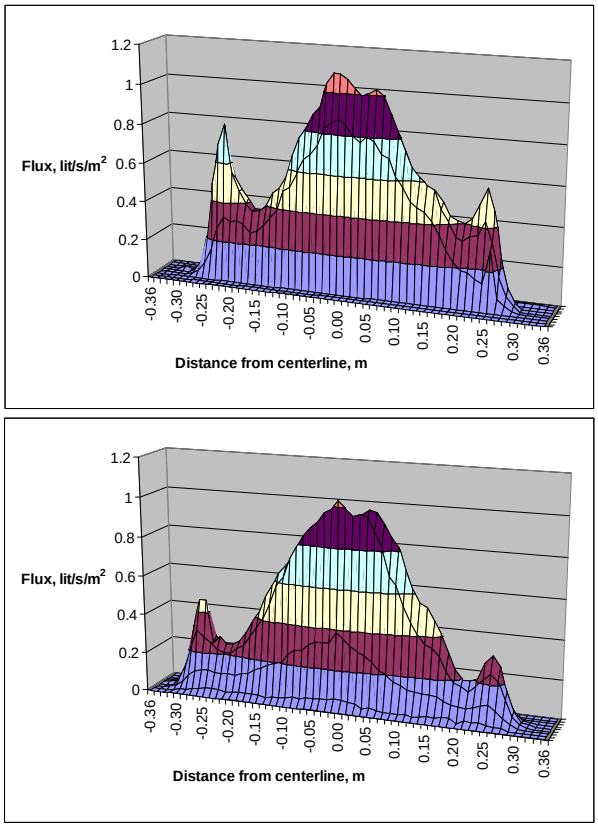

Figure 7. Patternation result for 8002 nozzle with flow conditions same as Figure 5. Top plot, water only. Bottom plot, with 1000 ppm InterLock® emulsion.

Figure 8, Figure 9, and Figure 10 show analogous data to Figure 5, Figure 6, and Figure 7, but this time for the AI9502 nozzle. Similar trends are evident. Figure 8 clearly shows that the emulsion again causes a retraction in the sheet disintegration region.

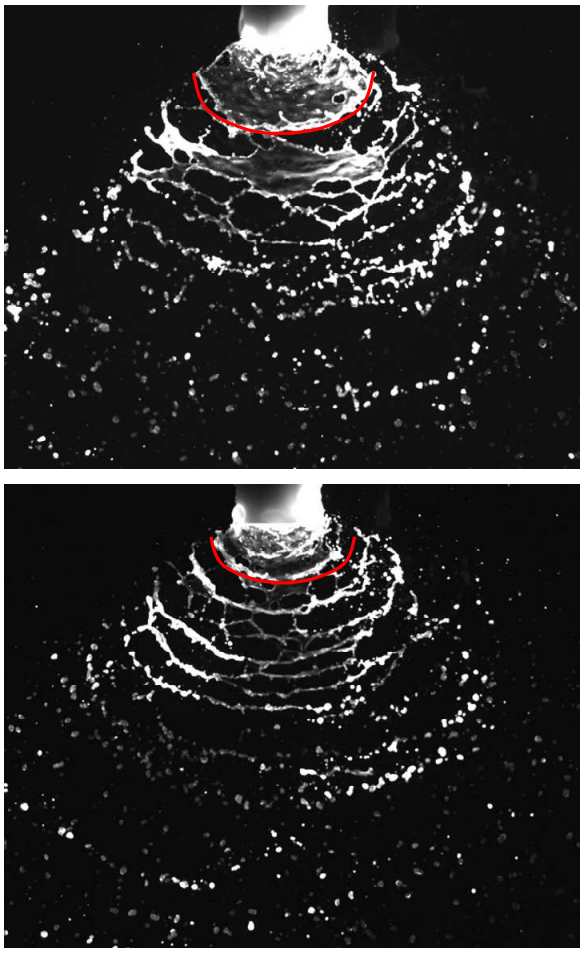

Figure 8. Sample images at 40 psi backpressure backpressure (flow 1.26×10^{-5} m^3/s) with the AI9502 nozzle. Top image, water only. Bottom image, with 1000 ppm InterLock® emulsion. Red lines annotate approximate boundary of initial sheet disintegration.

Figure 9 shows a broadening of the velocity contours, though much less distinct than the 8002 case.

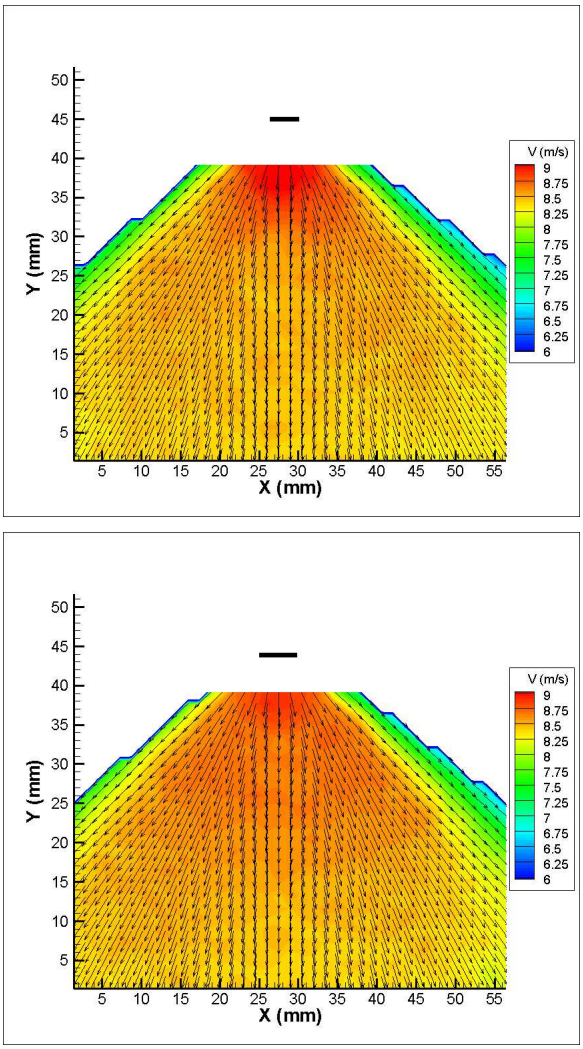

Figure 9. Velocity vectors with contour plot colored by velocity magnitude for AI9502 nozzle with flow conditions same as Figure 8. Top image, water only. Bottom image, with 1000 ppm InterLock® emulsion.

Figure 10 shows patternation results. The emulsion effect again is to reduce the fraction of the spray at the outer boundaries.

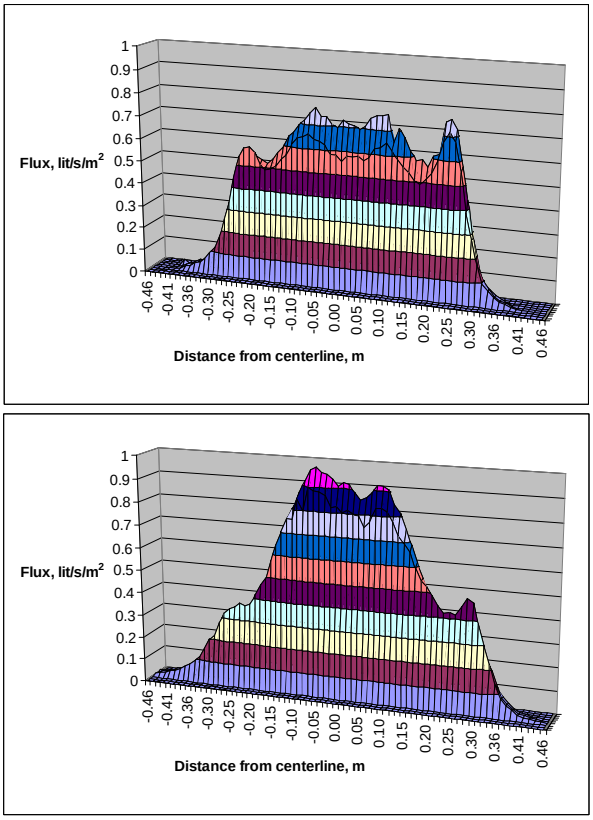

Figure 10. Patternation result for AI9502 nozzle with flow conditions same as Figure 8. Top plot, water only. Bottom plot, with 1000 ppm InterLock® emulsion.

In order to compare the performance of the nozzles, several attributes were calculated for each case. First and foremost, the driftable fines were calculated from the drop size distribution. The definition of the mass fraction of driftable fines, x_{fines}, was taken to be that of droplets less than 100 µm. The fines were measured 12" from the nozzle tip, along the center line of the spray. Table 1 shows the calculated results.

The average breakup length, L_B, was calculated directly from the PLIF images. It is defined as the distance from the nozzle tip to a point where the sheet is completely broken apart over the entire spray angle. Initial holes in the sheet that start in a region but not propagated to the edges are not counted in this definition of L_B. See Figure 11 for an illustration of how L_B is calculated. Normally L_B falls along the centerline of the spray. Table 1 shows the L_B calculated in this study.

The measurement of L_B and the known velocity profiles shown in Figure 6 and Figure 9 can be combined to calculate the breakup time, t_B. The t_B is a characteristic processing time of spray atomization and is shown in Table 1 as well. The t_B is controlled by the nozzle design.

Attribute	8002	AI9502
x_{fines}, water only	0.190	0.018
x_{fines}, emulsion	0.047	0.013
% reduction in x_{fines} due to emulsion	75	28
d_{32}, water only, µm	150	360
d_{32}, emulsion, µm	230	380
D_{50}, water only, µm	180	510
D_{50}, emulsion, µm	200	490
L_B, water only, mm	27 ± 2	14 ± 2
L_B, emulsion, mm	16 ± 2	10 ± 2
% reduction in L_B due to emulsion	40	30
t_B, water only, ms	1.28 ± 0.08	1.6 ± 0.3
t_B, emulsion, ms	0.78 ± 0.07	1.2 ± 0.3
% reduction in t_B due to emulsion	40	25

Table 1. Measurements of fines from dynamic image analysis and sheet disintegration from PLIF spray tests.

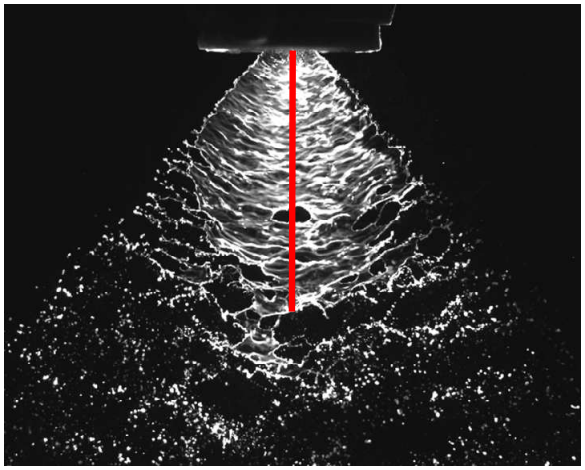

Figure 11. Example image showing the definition of the breakup length L_B.

Table 1 shows the dramatic reduction in x_{fines} due to the emulsion. This effect is shown for both types of nozzles, although is more pronounced for the 8002. A comparison between the two nozzle types shows that the AI9502 nozzle produced about an order of magnitude less driftable fines than the 8002 without the emulsion.

Table 1 shows also the significant reduction in L_B caused by the emulsion. This occurs for both nozzle types. The table shows that the air induction nozzle has a significantly smaller breakup length than the 8002 style. Similarly, the breakup time t_B is reduced by the emulsion. Due to the much smaller average velocity from the air injection nozzle, the AI9502 breakup time is actually higher than the 8002.

A schematic on a plausible reason for the earlier sheet disintegration is shown in Figure 12. It is thought that the emulsion droplets are deformed by the shear field in the nozzle, and in the process of retraction, this causes fluctuations that ultimately serve to break up the sheet earlier (closer) to the nozzle tip. It is known from parallel experimentation in the authors' lab that the addition of small *solid* particles do not cause early disintegration such as was illustrated in Figure 5 [7]; the additive particles must be fluidic for this effect to occur .

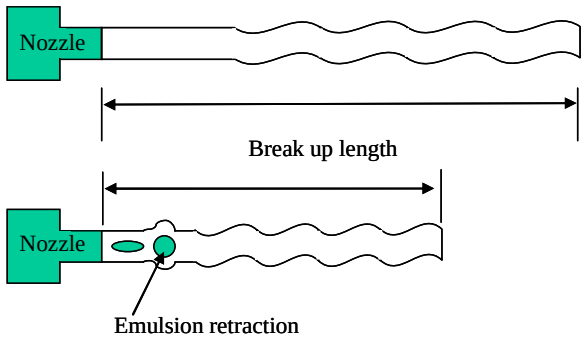

Figure 12. Proposed mechanisms for spray break up without emulsion (top) and with emulsion (bottom).

By continuity arguments, the spreading unbroken sheet must thin out as it grows more distant from the nozzle tip. Hence a disintegration that starts closer to the tip would occur with a larger thickness dimension in the sheet and therefore larger droplets can be expected.

Turbulence characteristics can be helpful in understanding nozzle performance. The Reynolds number based on the average velocity and minimum dimension of the elliptical nozzle is 10300, showing that turbulence indeed occurs in the outlet region. The shear rate in an elliptical nozzle such as the 8002 has been estimated [6] as $2\text{x}10^5$ to $6\text{x}10^5$ s^{-1} at 40 psi pressure drop, depending on the location in the elliptical exit. The hydraulic power is calculated as

$$P = \Delta p \dot{V} = \Delta p \frac{\dot{m}}{\rho} \qquad (1)$$

which, after subtracting out acceleration effects ($\frac{1}{2}\rho V^2$), for the 8002 nozzle results in 1.3 W. The volume over which the remaining pressure is dissipated is difficult to estimate but as a minimum it is the volume of the restricted region inside the nozzle, near 0.3 cm^3. The energy dissipation rate (power per mass), ε, is then calculated to be near 3000 W/kg.

The turbulence (Kolmolgorov) microscale, η, and time scale t_η are related to the momentum diffusivity and energy dissipation rate [8]:

$$\eta = \left(\frac{\nu^3}{\varepsilon} \right)^{1/4} \qquad (2)$$

$$t_\eta = \left(\frac{\nu}{\varepsilon} \right)^{1/2} \qquad (3)$$

where ν is the kinematic viscosity. The η is the length scale of the smallest turbulent eddies, while the t_η is associated with the lifetime of those eddies.

From Equation (2) the turbulence microscale is calculated to be near 4 µm for the stated ε. With the aforementioned D_{50} of the emulsion droplets at 16 µm, it is quite plausible that the structure of the turbulence at small scales interacts directly with the emulsion droplets near the nozzle tip. From Equation (3) the turbulence timescale t_η is near 20 µs, about fifty times less than the breakup time, implying that the role of turbulence in droplet deformation occurs very early in the breakup process.

From the data compiled by Grace [9], for dispersed-to-continuous viscosity ratios μ_d/μ_c greater than about 3.5, drops can not be broken by simple shear in the continuous phase due to the viscous resistance by the drops. With the viscosity ratio of this study being 5.3, no breakage due to simple shear is expected, however it could well contribute to deformation.

A large contribution from extensional shear is expected for these spray configurations. For this condition, Grace [9] shows that the Capillary number is 0.3 for the critical (maximum stable) droplet size at the viscosity ratio of interest:

$$Ca = \frac{\mu_c G d_{\max}}{2\sigma} \qquad (4)$$

where G is the shear rate, d_{max} is the maximum stable drop size in the emulsion, and σ is the interfacial tension. For the stated shear rate range, taking Ca to be 0.3 and σ estimated at 0.005 N/m, d_{max} is calculated to be in the range of 5 to 15 µm. Hence, deformation and possibly some breakup of emulsion droplets can be expected. In reference [7], it is shown that emulsion droplets with D_{50} near 10 µm show a broadening of the span with spraying through the 8002, although the median remains about constant. In the same study, two separate smaller sized emulsions (D_{50} equals 0.1 µm and 5 µm) showed almost no change in emulsion size distribution upon spraying, consistent with the d_{max} calculation. The driftable fines were reduced by all the emulsions tested. Hence the mechanism of Figure 12 remains plausible; though breakup cannot be ruled out in some systems tested, it is not an overriding factor.

For AI nozzles, the air as fluid can in principle also have an effect as described in Figure 12. This may well contribute to why the nozzles have such an early sheet disintegration as compared to the 8002 even without the emulsion present.

Other attributes of the spray disintegration were calculated including the wavelength λ_B of initial ligaments formed after breakup and the corresponding time period, P_B, and frequency, ν_B, between the ligaments. These results are shown in Table 2. The P_B was calculated from the wavelength divided by the local velocity.

Attribute	8002	AI9502
λ_B, mm, water only	2.5 ± 0.4	3.4 ± 0.8
λ_B, mm, emulsion	2.0 ± 0.3	2.7 ± 0.7
% reduction in λ_B due to emulsion	20	20
P_B, µs, water only	120 ± 20	390 ± 90
P_B, µs, emulsion	90 ± 10	320 ± 80
% reduction in P_B due to emulsion	30	20
ν_B, s^{-1}, water only	8500 ± 1300	2600 ± 600
ν_B, s^{-1}, emulsion	11000 ± 1700	3100 ± 600

Table 2. Measurements on ligament characteristics from PLIF spray tests

The table shows that the wavelength of the ligaments is reduced by the emulsion, as is the period. The AI9502 nozzle has a larger wavelength and period than does the 8002 nozzle. The time period between the ligaments is an order of magnitude smaller than the breakup timescale, i.e. ~ 1000 µs vs. ~100 µs, but still an order of magnitude higher than the turbulence timescale.

Conclusions

1. The InterLock® oil-in-water emulsion reduces fines for all of the spray nozzles tested.
2. Sheet disintegration is the prevailing mechanism of droplet formation. When the oil phase was present, an earlier breakup of the sheet, closer to the nozzle tip, is clearly seen. In the images, a breakup period is visible near the breakup area which could be translated to a wavelength and frequency. The frequency increases with the oil phase present, consistent with an earlier breakup.
3. The InterLock® had a marked influence on both the spray pattern (measured via patternation) and velocity profile (via PLIF), particularly for the 8002. For the nozzles tested, the effect was to

move the mass from the outer portions to the center of the spray.

4. The AI9502 nozzle was found to give a significantly smaller driftable fines fraction than the 8002 nozzle, both with and without the oil phase present. The average velocity of droplets for the AI9502 nozzle is less than half that of the 8002. The AI9502 breakup length was found to be lower than the 8002, however the breakup time was higher.
5. The length of the turbulence microscale suggests that the smallest eddies can interact with the emulsion droplets. The 20 µs turbulence timescale suggests that the role of turbulence in influencing sheet disintegration occurs very near the nozzle tip.
6. The effect of the emulsion on the spray behavior is explained by the ability of the oil droplets to oscillate and impact disintegration frequency, resulting in an earlier sheet disintegration. A similar role may be played by air bubbles incorporated into the fluid by air induction nozzles.

Nomenclature

Ca	Capillary number, defined by eqn. (4)
d_{32}	Sauter mean drop size, µm
D_{50}	volume median drop size, µm
D_{90}	diameter of the particles below which 90% of the mass is present, µm
d_{max}	maximum stable drop size, µm
L_B	Breakup length, mm
P_B	period between ligaments, µs
t_B	Breakup time, ms
t_η	time scale of microscale turbulence, ms
V	spray velocity, m/s
x_{fines}	mass fraction of driftable fines, defined to be droplets less than 100 µm
ε	energy dissipation rate, W/kg
η	turbulence microscale, µm
λ_B	wavelength of ligaments, m
μ_c	continuous phase viscosity, Pa-s
μ_d	dispersed phase viscosity, Pa-s
ν	kinematic viscosity, m^2/s
ν_B	frequency of ligaments near breakup region, s^{-1}
ρ	liquid density, kg/m^3
σ	interfacial tension, N/m

References

1. M. Raffel, C.E. Willert, and J. Kompenhans, *Particle Image Velocimetry. A Practical Guide*, Springer-Verlag, Berlin, 1998.
2. E.L. Paul, V.A. Atiemo-Obeng, S.M. Kresta, *Handbook of Industrial Mixing*, p. 237. John Wiley & Sons, Inc., Hoboken, NJ, 2004.
3. G.Pan, H. Meng, *AIChE Journal*, 47:2653-2665, 2001.
4. B.F. Bai, H.B. Zhang, L. Liu, H.J. Sun, *Experimental Thermal and Fluid Science*, 33:1012-1020, 2009.
5. Y.Yan, S. Gashi, J.M. Nouri, R.D. Lockett, C. Arcoumanis, *Journal of Physics: Conference Series*, 85, 2007.
6. H. Zhu, R.D. Brazee, D.L. Reichard, R.D. Fox, C.R. Krause, and A.C. Chapple, *Atomization and Sprays*, 5:343-356, 1995.
7. K. Qin, H. Tank, S. Wilson, B. Downer, L. Liu, *Atomization and Sprays*, in press.
8. S.B. Pope, *Turbulent Flows*, p. 128, Cambridge University Press, 2001
9. H.P. Grace, *Chemical Engineering Communications*, 14:225-277, 1982.